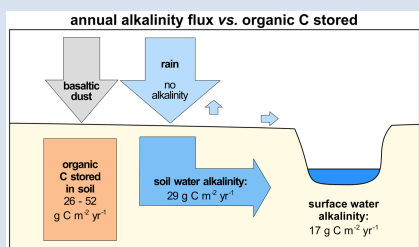


## ■ Direct evidence of CO<sub>2</sub> drawdown through enhanced weathering in soils

T. Linke<sup>1\*</sup>, E.H. Oelkers<sup>1,2</sup>, S.C. Möckel<sup>3</sup>, S.R. Gislason<sup>1</sup>



### Abstract



The ability of engineered enhanced weathering to impact atmospheric CO<sub>2</sub> has been challenging to demonstrate due to the many processes occurring in soils and the short time span of current projects. Here we report the carbon balance in an Icelandic Histic/Gleyic Andosol that has received large quantities of basaltic dust over 3300 years, providing opportunity to quantify the rates and long term consequences of enhanced weathering. The added basaltic dust has dissolved continuously since its deposition. The alkalinity of the soil waters is more than 10 times higher than in equivalent basalt dust-free soils. After accounting for oxidation and degassing when the soil waters are exposed to the atmosphere, the annual CO<sub>2</sub> drawdown due to

alkalinity generation is 0.17 t C ha<sup>-1</sup> yr<sup>-1</sup>. This study validates the ability of fine grained mafic mineral addition to soils to attenuate increasing atmospheric CO<sub>2</sub> by alkalinity export. Induced changes in soil organic carbon storage, however, likely dominate the net CO<sub>2</sub> drawdown of enhanced weathering efforts.

Received 25 October 2023 | Accepted 17 March 2024 | Published 30 April 2024

### Introduction

The natural weathering of basaltic and ultramafic rocks has been demonstrated to have a relatively large role in the drawdown of CO<sub>2</sub> from the atmosphere (Dessert *et al.*, 2003; Gislason *et al.*, 2009; Taylor *et al.*, 2021). Such observations have motivated several proposals to use these rocks to remove CO<sub>2</sub> directly from the atmosphere through a process called Enhanced Weathering (EW) (Moosdorf *et al.*, 2014; IPPC, 2018; Beerling *et al.*, 2020). Enhanced weathering involves amending soils with crushed fine grained, fast reacting Ca-Mg silicate rocks and minerals such as basalts and peridotites (Strelfer *et al.*, 2018). To date, enhanced weathering field experiments have demonstrated improved crop vigour, organic and inorganic carbon storage and decreased N<sub>2</sub>O degassing (Haque *et al.*, 2019a, 2020; Beerling *et al.*, 2020). One of the goals of EW is to increase the alkalinity export of waters that drain from soils and enter rivers and streams. The quantification of carbon drawdown by enhanced weathering has been challenging to identify or quantify due to the large number of processes that occur in soils and the short duration of existing field studies.

One approach to investigate the long term behaviour and consequences of EW is *via* natural analogues. Enhanced weathering experiments to date have tested the addition of up to 400 t ha<sup>-1</sup> yr<sup>-1</sup> of crushed Ca-Mg silicate rocks to agricultural soils (Gillman *et al.*, 2002; Amann *et al.*, 2018; Haque *et al.*, 2019b). This crushed rock flux is orders of magnitude higher than the average global desert dust deposition on Earth, which is estimated to be 0.5 t ha<sup>-1</sup> yr<sup>-1</sup> (Mahowald *et al.*, 2005). In the vicinity

of the dust "hot spots", such as South Iceland, however, the mass of deposited fine grained basaltic dust can be as high as 8 t ha<sup>-1</sup> yr<sup>-1</sup> (Arnalds, 2010; Arnalds *et al.*, 2014, 2016). Although this natural mass flux of basalt is less than that of current EW efforts, 1) this basaltic dust flux has been added continuously to the soil of this region over at least the past 3300 years, such that in total over 16,500 t ha<sup>-1</sup> of basaltic dust has been added over this time, and 2) the specific surface area of natural basaltic dust is likely higher than that added to soils in current EW experiments due to its finer grain size. The grain size of the crushed rocks used in EW applications, if reported, is commonly less than 150 µm (Haque *et al.*, 2019a; Gillman *et al.*, 2002). In contrast, the average size of basaltic Icelandic dust ranges from 10 to 62 µm (Arnalds *et al.*, 2014; Liu *et al.*, 2014). For these reasons, the mineral rich Histic/Gleyic Andosols (Arnalds, 2015) considered in this study located in South Iceland provide an insightful natural analogue to illuminate the long term effect of EW applications performed under similar climate, vegetation, and soil conditions. The studied soil receives large amounts of air borne volcanic material during 1) explosive volcanic eruptions in the form of glassy volcanic ash fallout, and 2) dust storms (Shoji *et al.*, 1995; Arnalds *et al.*, 2016). Explosive eruptions lead to evident tephra horizons that can be used to date these soils. The more frequently deposited windblown dust is finer grained than the tephra and intermingled with the soil organic carbon (see "Soil classification and soil evolution in Iceland" in Supplementary Information). Based on palaeoecologic research (Gísladóttir *et al.*, 2008; Arnalds, 2015; Möckel *et al.*, 2017), in the absence of volcanic dust input, the Histic/Gleyic Andosols of

1. Institute of Earth Sciences, University of Iceland, Sturlugata 7, 102 Reykjavik, Iceland

2. Ali I. Al-Naimi Petroleum Engineering Research Center, KAUST, Saudi Arabia

3. Institute of Life and Environmental Sciences, University of Iceland, Sturlugata 7, 102 Reykjavik, Iceland

\* Corresponding author (email: tol5@hi.is)



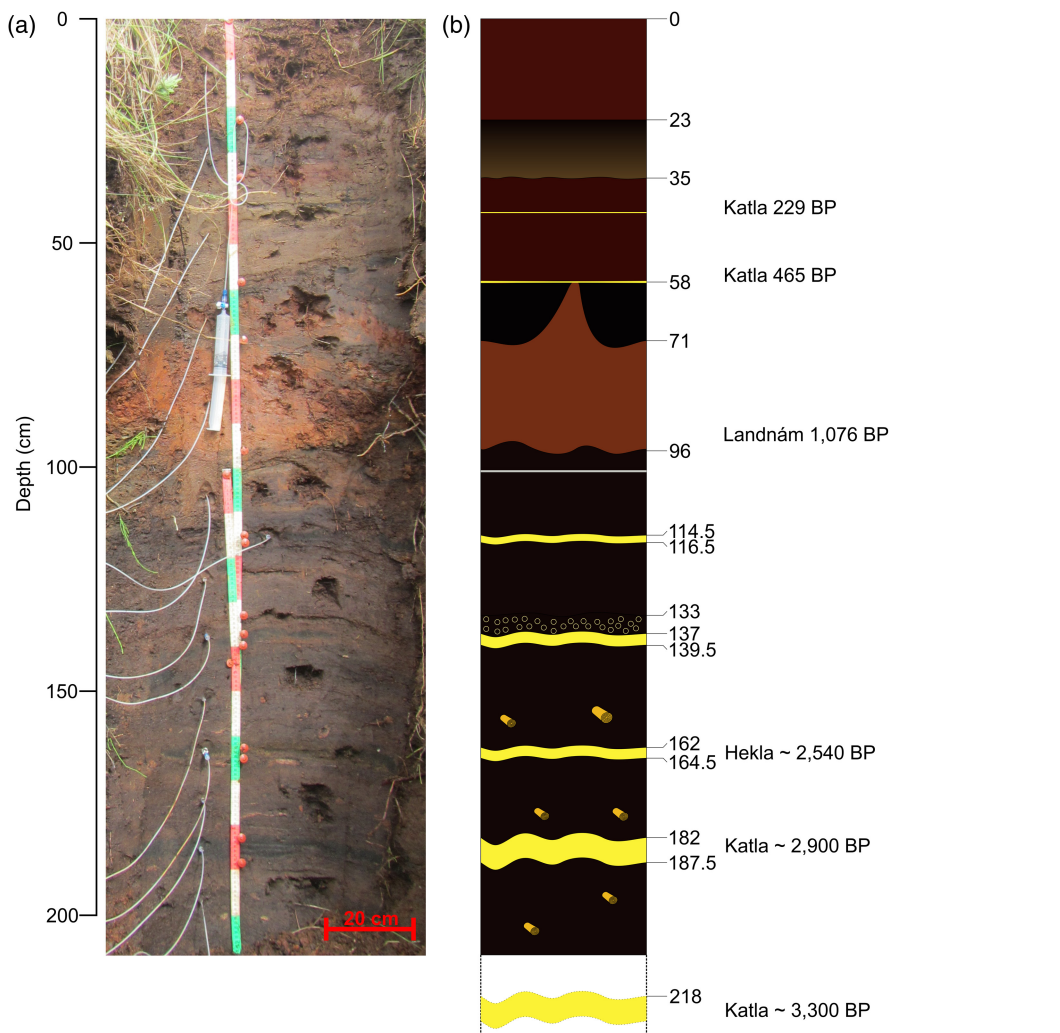


**Figure 1** (a) Photograph of the studied soil system. The dark layers correspond to tephra originating from historic volcanic eruptions. (b) Schematic illustration of the soil profile with depths and ages (in years before present) of identified tephra layers shown in yellow for better visibility, the Landnám Layer that occurred around the time of the Icelandic settlement could not be clearly identified because of alteration. Plant remnants are visible in the lower part of the profile, indicating high organic content.

Southern Iceland would have developed into Histosols (Arnalds, 2008). Consequently, the comparison of the behaviour of South Icelandic Histic/Gleyic Andosols with that of volcanic dust-free Histosols, located in similar climatic zones provides insight into the consequences of adding fine grained basaltic material to soils as part of enhanced weathering efforts.

One of our motivations to focus on the addition of volcanic material to Histosols/peat soils to drawdown CO<sub>2</sub> from the atmosphere stems from the role of these soils in the global carbon cycle. Although peatlands cover only about 3 % of the continents (Xu et al., 2018), they store ~10 % of all non-glacial freshwater and roughly 30 % of the land-based organic carbon (Mitra et al., 2005; Bragazza et al., 2013). Man made drainage and burning of peat areas worldwide releases 0.5–0.8 Gt C yr<sup>-1</sup>, which is equivalent to 5–8 % of global anthropogenic carbon emissions (Hooijer et al., 2006; Parish et al., 2008). Carbon dioxide emission from the drainage of peat areas is estimated to be the largest anthropogenic source of CO<sub>2</sub> emissions in Iceland (Keller et al., 2020). The addition of reactive silicate rock dust to peat soils might help increase carbon storage being otherwise lost due to peatland draining.

This manuscript is one of two exploring the long term efficiency and consequences of enhanced rock weathering efforts

through the study of a South Iceland Gleyic/Histic Andosol. The first manuscript (Linke et al., 2024) reports the composition of fluids and solids collected over two field seasons to 1) quantify the saturation state of the primary and secondary mineral phases with respect to the soil solutions, 2) determine the processes controlling the mobility of heavy metals, and 3) assess the rate at which basalt dissolved in the soils. In this manuscript we present a comparison of the alkalinity export from this soil with corresponding results from volcanic dust-free Histosols to quantify the ability of enhanced weathering efforts to drawdown CO<sub>2</sub> from the atmosphere. Results are then used to estimate the efficiency of enhanced weathering at a larger scale. The purpose of this paper is to present the results of this study and use the results to gain insight into the consequences of current and future enhanced weathering efforts.

## Field Site Description

The field site is located above the source of the Rauðalækur ("Red creek") river at 63° 53' 42.5" N, 20° 21' 15.9" W, which is approximately 7 km north of the town of Hella in South Iceland. This site consists of an upper Gleyic Andosol and a lower Histic Andosol (see Supplementary Information for further

details). The study site receives an annual aeolian dust flux of 5–8 t ha<sup>-1</sup> yr<sup>-1</sup>, consisting of mostly basaltic glass (Arnalds *et al.*, 2016). Additional basaltic material is added during irregular volcanic events. During the past several decades, drainage trenches have been cut into the nearby soils; the closest drainage ditch is located more than 150 metres from the study site. The studied soil contains several prominent horizontal tephra layers, with thicknesses ranging from a few mm to few cm and deposited during the past 3300 years. An image and schematic illustration of the system is provided in Figure 1 and a detailed description of the field site is provided in the [Supplementary Information](#) and Table S-1 therein.

## Results

**Fluid compositions.** Soil fluid samples were collected using suction cup samplers from May to November 2018. The compositions of all fluid samples are provided in Table S-2 ([Supplementary Information](#)) and selected dissolved constituents are shown as a function of depth in Figure 2. The pH of the samples was recalculated using PHREEQC (Parkhurst and Appelo, 1999) to the *in situ* soil temperature of 7 °C. This is the average soil temperature at 76–260 cm depth during the summer months (Petersen and Gerber, 2018). The concentrations of major elements increase continuously with depth suggesting the continuous dissolution of the basaltic dust in the soil. The soil waters become increasingly anoxic with depth as indicated by the Eh values shown in Figure 2b.

The alkalinity of the soil waters increases from 0 to 3 meq kg<sup>-1</sup> with depth. Once these waters exit the soils, they will equilibrate with the O<sub>2</sub> and CO<sub>2</sub> in the atmosphere. PHREEQC calculations indicate that the alkalinity of the soil waters will decrease on average to 1.53 ± 0.2 meq kg<sup>-1</sup> due to iron oxidation/precipitation reactions when they come in contact with the atmosphere as they flow into local rivers (further details of this calculation are provided in the [Supplementary Information](#)).

The alkalinity of soil waters in our studied dust-rich soil are compared to the corresponding alkalinities of basalt

dust-free Histosols located in non-carbonate terrains in Figure 3. Our field site, mostly fed by rainwater, shows considerably higher alkalinity and pH values than observed in corresponding basalt dust-free Histosols. Histosols located in carbonate terrains are not included in this comparison as the presence of carbonate minerals leads to a pH and alkalinity increase due to carbonate dissolution, a process which has no long term net effect on atmospheric carbon drawdown. The comparison in Figure 3 shows that the addition of volcanic dust to our soil increased substantially the alkalinity in its soil waters, most notably deep in the soil column. This observation confirms the ability of enhanced weathering by the addition of basaltic dust to soils to drawdown CO<sub>2</sub> from the atmosphere.

A noteworthy observation is that the basaltic dust in the studied soil column persists and is reactive throughout the soil column, despite the fact that some of this dust has been present in the soil for 3300 years. This observation is consistent with mass balance estimates of the import and export of metals to the soil column. The study site receives an average annual dust flux of 500–800 g m<sup>-2</sup> yr<sup>-1</sup>. This basalt flux adds 0.96–1.54 mol Ca and 0.72–1.16 mol Mg per m<sup>2</sup> yr<sup>-1</sup> to the soil. In contrast, the average Ca and Mg concentration of the deep soil water is 5 × 10<sup>-4</sup> and 4 × 10<sup>-4</sup> mol kg<sup>-1</sup> for Ca and Mg, respectively. Taking account of the estimated 925 ± 150 kg m<sup>-2</sup> yr<sup>-1</sup> of water that flows through, and is exported annually by our studied soil (see [Supplementary Information](#) for details of this water flow estimate), we estimate that 0.47 ± 0.07 and 0.37 ± 0.06 mol yr<sup>-1</sup> of Ca and Mg, respectively, are removed from the soil per square metre of soil surface area at present. The input of Ca and Mg by volcanic dust addition is, therefore, approximately 2–3 times more than that removed by soil water export. The results of this comparison are consistent with the persistence of the reactive dust throughout the soil column and suggest the long term viability of enhanced weathering efforts.

**Carbon Storage via alkalinity export by the addition of basaltic material to soils.** The rate of carbon drawdown due to alkalinity export by enhanced weathering in our studied field site can be estimated by combining the annual water flux through the soil and the measured alkalinity, as demonstrated in

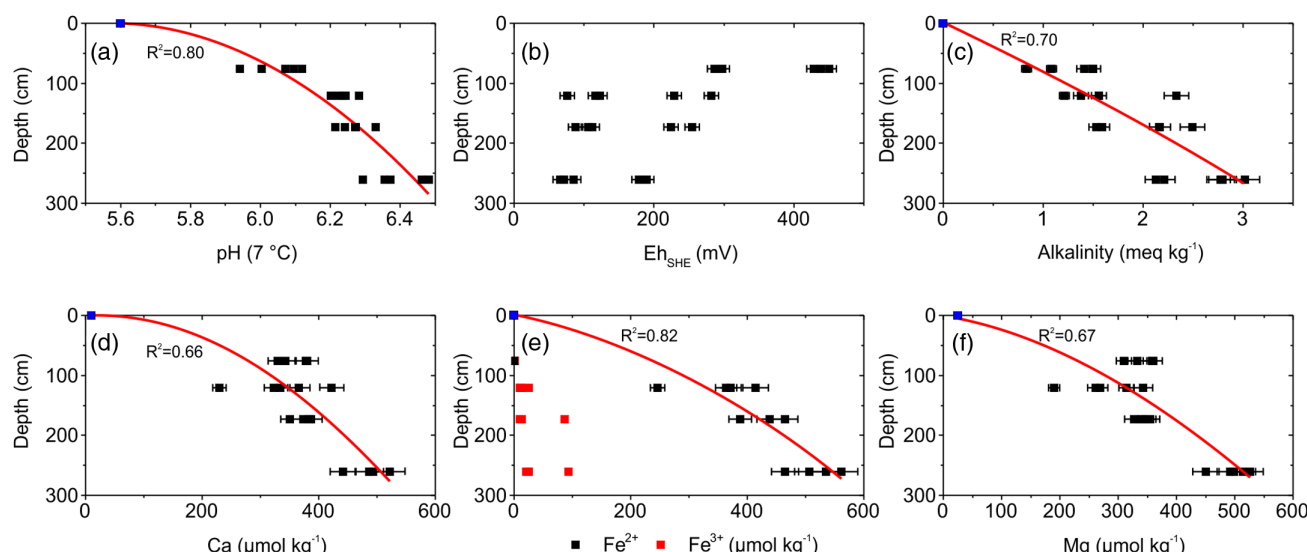


**Figure 2** Measured soil water concentrations determined in the present study in all samples collected from May to November 2018, as a function of depth. The pH values are normalised to a 7 °C reference temperature and Eh values to a Standard Hydrogen Electrode. The black squares represent measured water concentrations, whereas the blue squares show the composition of rainwater. The error bars correspond to a ±5 % uncertainty on the measured concentrations; error bars do not appear if the uncertainty is smaller than the symbol size. The red curves in the figure show 2<sup>nd</sup> order polynomial fits of all the measured concentrations with the corresponding R<sup>2</sup> values next to each curve.

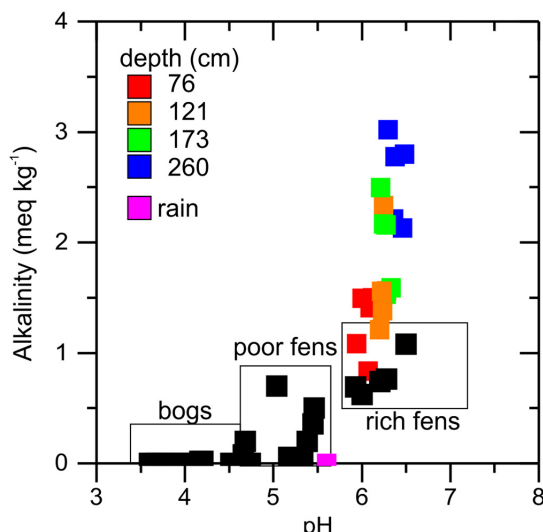


**Figure 3** Comparison of pH and alkalinity of soil waters collected from our studied soil with similarly composed, but volcanic dust-free soils reported in other studies. The black symbols correspond to alkalinity values reported in the literature for Histosols from bogs, poor or rich fens located in non-volcanic regions and in the absence of carbonate bedrock. The black boxes around the black symbols represent the commonly reported pH-alkalinity ranges of bogs and fens respectively. The red, orange, green and blue symbols represent soil water samples measured in the present study at the depths indicated in the figure. The purple symbol shows the composition of rainwater at our field site. The sources and location of the literature data are provided in Table S-3 of the Supplementary Information.

**Figure 4.** By taking account of the rainfall, evaporation, and surface runoff it is estimated that  $925 \pm 150 \text{ kg m}^{-2} \text{ yr}^{-1}$  of water pass through and are exported from the studied soil annually. Multiplying this number by the  $1.53 \pm 0.2 \text{ meq kg}^{-1}$  average alkalinity of the deepest water samples of our study area, after its equilibration with the atmosphere, yields an estimated alkalinity export from our soils of  $1.43 \pm 0.3 \text{ meq m}^{-2} \text{ yr}^{-1}$ . Multiplying this number by the atomic weight of carbon yields an annual carbon addition to our river water of  $17 \pm 3.6 \text{ g m}^{-2} \text{ yr}^{-1}$ , which equals  $0.17 \pm 0.036 \text{ t ha}^{-1} \text{ yr}^{-1}$  of C. The degree to which this carbon drawdown rate is influenced by the rate of basalt input to the soil and its surface area has yet to be quantified. Although, dissolution rates are commonly thought to be proportional to the fluid-mineral surface area, these rates are also influenced by fluid compositions, including approach to equilibrium and fluid flow paths in the soil column (Schott *et al.* 2009; Linke *et al.* 2024).

It is insightful to extrapolate this annual rate of carbon drawdown to a larger scale. If the results of our studied field site are representative, the removal of  $1 \text{ Gt yr}^{-1} \text{ CO}_2$  from the atmosphere through alkalinity production would require a total of 16 million km<sup>2</sup> of surface. This is larger than the total surface area of the United States. Moreover, the mass of basaltic dust required to provoke this rate of carbon removal may be unrealistically large. The average annual flux of basaltic dust into the studied South Iceland soils is  $5\text{--}8 \text{ t ha}^{-1} \text{ yr}^{-1}$ . Adding this mass of basalt over 16 million km<sup>2</sup> of surface would require 8 to 13 Gt of finely ground basalt annually. This mass of ground basalt is larger than the world's annual cement production of 4.3 Gt in 2020 (<https://iea.org/reports/cement>). This conclusion, based on the alkalinity export from our studied soil, which contains more organic matter (12 % to >20 % C) than most soils globally (<5 % C; e.g., Stockmann *et al.* 2015), is nevertheless supported

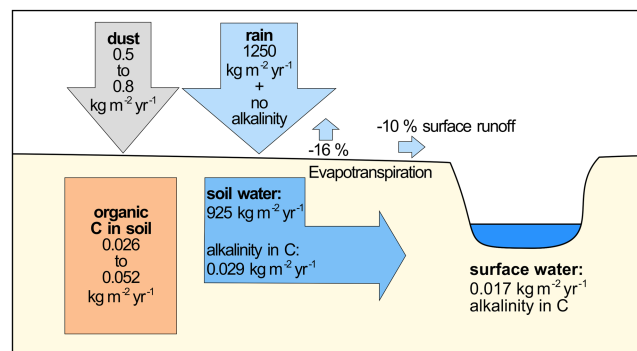


**Figure 4** Schematic illustration of the processes drawing down  $\text{CO}_2$  at our field site. The site receives  $\sim 1250 \pm 200 \text{ kg m}^{-2} \text{ yr}^{-1}$  of rainfall. Of this rainfall 16 % is estimated to evaporate and 10 % is estimated to be lost to surface runoff. As the remaining  $925 \pm 150 \text{ kg m}^{-2} \text{ yr}^{-1}$  of water passes through the soil, its alkalinity increases on average from 0 to  $2.59 \pm 0.34 \text{ meq kg}^{-1}$  at depth. Once these waters equilibrate with the atmosphere, this fluid oxidises and some  $\text{CO}_2$  is released such that the alkalinity decreases to  $1.53 \pm 0.2 \text{ meq kg}^{-1}$  resulting in an annual export of  $17 \pm 3.6 \text{ g C per m}^2 \text{ soil surface area}$ . At the same time  $26\text{--}52 \text{ g m}^{-2} \text{ yr}^{-1}$  of C is drawn down from the atmosphere by organic carbon production and stored in the soil.

by other recent enhanced rock weathering studies. Our result of  $0.17 \pm 0.036 \text{ t ha}^{-1} \text{ yr}^{-1}$  of carbon drawdown from alkalinity export by enhanced rock weathering is within the range of the handful of large scale cropland EW studies of  $0.0005\text{--}0.5 \text{ t C ha}^{-1} \text{ yr}^{-1}$  (Haque *et al.*, 2020; Taylor *et al.*, 2021; Larkin *et al.*, 2022). It should be noted, however, that the alkalinity generated in our studied Histic/Gleyic Andosol was the consequence of the dissolution of the basalt added to this soil annually over the past 3300 years. This annual addition has led to a buildup of basaltic material over time. The results shown in Figure 2 indicate that the presence of older basaltic dust, located deep in the soil profile is an important contributor to alkalinity production. As such, it seems likely that substantially more than  $5\text{--}8 \text{ t ha}^{-1} \text{ yr}^{-1}$  would need to be added to soils near-term as part of enhanced weathering efforts to provoke a similar rate of alkalinity production as observed in our study area.

**Carbon drawdown by alkalinity production versus soil organic carbon.** The total mass of organic carbon in our studied soil is estimated to be  $86\text{--}172 \text{ kg C m}^{-2}$  with average net annual rate of carbon drawdown estimated to be  $26\text{--}52 \text{ g C m}^{-2} \text{ yr}^{-1}$  (see Supplementary Information). This rate of  $\text{CO}_2$  drawdown is substantially larger than the corresponding  $17 \pm 3.6 \text{ g C m}^{-2} \text{ yr}^{-1}$  drawdown due to alkalinity export in our studied soils. These estimates are in agreement with previous studies (Taylor *et al.*, 2021). These estimates also suggest that the amount of  $\text{CO}_2$  removed by the addition of basaltic dust to the soil in one year by alkalinity export is more than 3 orders of magnitude less than the total  $\text{CO}_2$  stored as organic carbon in the soil. This latter observation should serve as a warning to those attempting atmospheric  $\text{CO}_2$  drawdown by enhanced weathering in soils. If the addition of basaltic dust to soil leads to the accelerated decomposition of organic material in soils, the latter process could readily dominate leading to a net increase of  $\text{CO}_2$  released to the atmosphere due to enhanced weathering efforts.

## Conclusions

The results of this study confirm the ability of fine grained basaltic rock added to soils to enhance  $\text{CO}_2$  drawdown directly from the atmosphere due to alkalinity production. It is estimated

that  $17 \pm 3.6 \text{ g C m}^{-2} \text{ yr}^{-1}$  is currently drawn down and added to rivers by alkalinity production from our South Iceland field site. The enhanced alkalinity production of our soils was produced by the addition of approximately  $1.7\text{--}2.6 \text{ t m}^{-2}$  of basaltic dust to this soil over 3300 years. Upscaling of this process to address even a small fraction of the mass of anthropogenic CO<sub>2</sub> emissions to the atmosphere, however, may be challenging because 1) this enhanced weathering process is slow and would require more land than is available for a sizeable drawdown of CO<sub>2</sub> through alkalinity production, and 2) the currently unquantified effect of adding basalt powder to soils on soil organic matter. So, although this study demonstrates the potential of enhanced weathering efforts to contribute to attenuating atmospheric CO<sub>2</sub> concentrations, the degree to which this approach will prove successful at a larger scale remains unclear.

## Acknowledgements

The authors thank Knud Dideriksen for his comments and discussions during the field work. We thank the Icelandic meteorological office (Veðurstofa Íslands) for providing rainwater data, Liane Benning and the interface geochemistry group at the Geological research centre GFZ Potsdam for the DOC measurements, Þorsteinn Jónsson for assisting in the field and designing coring equipment and Egill Erlendsson and Guðrún Gísladóttir at University of Iceland for helping with site selection. We thank Bryndís Róbertsdóttir at the National Energy Authority Iceland for her help with identifying the tephra layers and Eiríkur Benjaminsson for access to his property. We thank Susan Stipp and Dominique Tobler, the Metal-Aid coordinators, as well as the network members for their pleasant company during this study. This project was funded by the European Union's Horizon 2020 research and innovation programme under the Marie Skłodowska-Curie grant agreement No 675219, from Landsvirkjun under the project number 2456, and the Icelandic Center for Research (Rannís) on behalf of the Doctoral Student Fund of the Ministry for the Environment and Natural Resources under the grant No 218929-051. Additional financial support was received from the Research Fund of the University of Iceland and the Travel grant for doctoral students at the University of Iceland. This research was partly supported by research grant CRG9 2020 KAUST-UI. SRG and EHO would like to thank Hussein Hoteit and Abdulkader M. Alafifi at KAUST University, Saudi Arabia for their hospitality and support.

*Editor:* Satish Myneni

## Additional Information

Supplementary Information accompanies this letter at <https://www.geochemicalperspectivesletters.org/article2415>.



© 2024 The Authors. This work is distributed under the Creative Commons Attribution 4.0 License, which permits unrestricted use, distribution, and reproduction in any medium, provided the original author and source are credited. Additional information is available at <http://www.geochemicalperspectivesletters.org/copyright-and-permissions>.

**Cite this letter as:** Linke, T., Oelkers, E.H., Möckel, S.C., Gislason, S.R. (2024) Direct evidence of CO<sub>2</sub> drawdown through enhanced weathering in soils. *Geochem. Persp. Let.* 30, 7–12. <https://doi.org/10.7185/geochemlet.2415>

## References

- AMANN, T., HARTMANN, J., STRUYF, E., DE OLIVEIRA GARCIA, W., FISCHER, E.K., JANSENS, I., MEIRE, P., SCHOEYNCK, J. (2018) Constraints on Enhanced Weathering and related carbon sequestration – a cropland mesocosm approach. *Biogeosciences Discussions* 1–21. <https://doi.org/10.5194/bg-2018-398>
- ARNALDS, O. (2008) Soils of Iceland. *Jökull* 58, 409–421. <https://doi.org/10.33799/jokull2008.58.409>
- ARNALDS, O. (2010) Dust sources and deposition of aeolian materials in Iceland. *Icelandic Agricultural Sciences* 23, 3–21.
- ARNALDS, O. (2015) *The Soils of Iceland*. World Soils Book Series, Springer, Dordrecht. <https://doi.org/10.1007/978-94-017-9621-7>
- ARNALDS, O., OLAFSSON, H., DAGSSON-WALDHAUSEROVA, P. (2014) Quantification of iron-rich volcanogenic dust emissions and deposition over the ocean from Icelandic dust sources. *Biogeosciences* 11, 6623–6632. <https://doi.org/10.5194/bg-11-6623-2014>
- ARNALDS, O., DAGSSON-WALDHAUSEROVA, P., OLAFSSON, H. (2016) The Icelandic volcanic aeolian environment: Processes and impacts — A review. *Aeolian Research* 20, 176–195. <https://doi.org/10.1016/j.aeolia.2016.01.004>
- BEERLING, D.J., KANTZAS, E.P., LOMAS, M.R., WADE, P., EUFRASIO, R.M., RENFORTH, P., SARKAR, B., ANDREWS, M.G., JAMES, R.H., PEARCE, C.R., MERCURE, J.-F., POLLITT, H., HOLDEN, P.B., EDWARDS, N.R., KHANNA, M., KOH, L., QUEGAN, S., PIDGEON, N.F., JANSENS, I.A., HANSEN, J., BANWART, S.A. (2020) Potential for large-scale CO<sub>2</sub> removal via enhanced rock weathering with croplands. *Nature* 583, 242–248. <https://doi.org/10.1038/s41586-020-2448-9>
- BRAGAZZA, L., PARISOD, J., BUTTLER, A., BARDGETT, R.D. (2013) Biogeochemical plant-soil microbe feedback in response to climate warming in peatlands. *Nature Climate Change* 3, 273–277. <https://doi.org/10.1038/nclimate1781>
- DESSERT, C., DUPRÉ, B., GAILLARDET, J., FRANÇOIS, L.M., ALLÈGRE, C.J. (2003) Basalt weathering laws and the impact of basalt weathering on the global carbon cycle. *Chemical Geology* 202, 257–273. <https://doi.org/10.1016/j.chemgeo.2002.10.001>
- GILLMAN, G.P., BURKET, D.C., COVENTRY, R.J. (2002) Amending highly weathered soils with finely ground basalt rock. *Applied Geochemistry* 17, 987–1001. [https://doi.org/10.1016/S0883-2927\(02\)00078-1](https://doi.org/10.1016/S0883-2927(02)00078-1)
- GÍSLADÓTTIR, G., ERLENDSSON, E., LAL, R., BIGHAM, J. (2008) Erosional Effects on Terrestrial Resources over the last Millennium in Reykjanes, Southwest Iceland. *Quaternary Research* 73, 20–32. <https://doi.org/10.1016/j.yqres.2009.09.007>
- GÍSLASON, S.R., OELKERS, E.H., EIRIKSDOTTIR, E.S., KARDJILOV, M.I., GÍSLADÓTTIR, G., SIGFUSSON, B., SNORRASON, A., ELEFSEN, S., HARDARDÓTTIR, J., TORSSANDER, P., OSKARSSON, N. (2009) Direct evidence of the feedback between climate and weathering. *Earth and Planetary Science Letters* 277, 213–222. <https://doi.org/10.1016/j.epsl.2008.10.018>
- HAQUE, F., SANTOS, R.M., DUTTA, A., THIMMANAGARI, M., CHIANG, Y.W. (2019a) Co-Benefits of Wollastonite Weathering in Agriculture: CO<sub>2</sub> Sequestration and Promoted Plant Growth. *ACS Omega* 4, 1425–1433. <https://doi.org/10.1021/acsomega.8b02477>
- HAQUE, F., CHIANG, Y., SANTOS, R. (2019b) Alkaline Mineral Soil Amendment: A Climate Change ‘Stabilization Wedge’? *Energies* 12, 2299. <https://doi.org/10.3390/en12122299>
- HAQUE, F., SANTOS, R.M., CHIANG, Y.W. (2020) CO<sub>2</sub> sequestration by wollastonite-amended agricultural soils – An Ontario field study. *International Journal of Greenhouse Gas Control* 97, 103017. <https://doi.org/10.1016/j.ijggc.2020.103017>
- HOOIJER, A., SILVIUS, M., WÖSTEN, H., PAGE, S. (2006) PEAT-CO<sub>2</sub>, Assessment of CO<sub>2</sub> emissions from drained peatlands in SE Asia. *Delft Hydraulic Report* Q3943.
- IPCC (2018) *Global warming of 1.5°C. An IPCC Special Report on the impacts of global warming of 1.5°C above pre-industrial levels and related global greenhouse gas emission pathways, in the context of strengthening the global response to the threat of climate change, sustainable development, and efforts to eradicate poverty*. MASSON-DELMOTTE, V., ZHAI, P., PÖRTNER, H.O., ROBERTS, D., SKEA, J., SHUKLA, P.R., PIRANI, A., MOUFOUMA-OUIKA, W., PÉAN, C., PIDCOCK, R., CONNORS, S., MATTHEWS, J.B.R., CHEN, Y., ZHOU, X., GOMIS, M.I., LONNOY, E., MAYCOCK, T., TIGNOR, M., WATERFIELD, T. (Eds.) World Meteorological Organization, Geneva, Switzerland. [https://www.ipcc.ch/site/assets/uploads/sites/2/2019/06/SR15\\_Full\\_Report\\_High\\_Res.pdf](https://www.ipcc.ch/site/assets/uploads/sites/2/2019/06/SR15_Full_Report_High_Res.pdf)
- KELLER, N., STEFANI, M., EINARSDÓTTIR, S., HELGADÓTTIR, A., GUÐMUNDSSON, J., SNORRASON, A., THORSSON, J., TINGANELLI, L. (2020) *National Inventory Report - Emissions of greenhouse gases in Iceland from 1990 to 2018*. The Environment Agency of Iceland, Reykjavík.



- LARKIN, C.S., ANDREWS, M.G., PEARCE, C.R., YEONG, K.L., BEERLING, D.J., BELLAMY, J., BENEDICK, S., FRECKLETON, R.P., GORING-HARFORD, H., SADEKAR, S., JAMES, R.H. (2022) Quantification of CO<sub>2</sub> removal in a large-scale enhanced weathering field trial on an oil palm plantation in Sabah, Malaysia. *Frontiers in Climate* 4, 959229. <https://doi.org/10.3389/fclim.2022.959229>
- LINKE, T., OELKERS, E.H., DIDERIKSEN, K., MÖCKEL, S.C., NILABH, S., GRANDIA, F., GISLASON, S.R. (2024) The geochemical evolution of basalt Enhanced Rock Weathering systems quantified from a natural analogue. *Geochimica et Cosmochimica Acta* 370, 66–77. <https://doi.org/10.1016/j.gca.2024.02.005>
- LIU, E.J., CASHMAN, K.V., BECKETT, F.M., WITHAM, C.S., LEADBETTER, S.J., HORT, M.C., GUÐMUNDSSON, S. (2014) Ash mists and brown snow: Remobilization of volcanic ash from recent Icelandic eruptions. *Journal of Geophysical Research: Atmospheres* 119, 9463–9480. <https://doi.org/10.1002/2014JD021598>
- MAHOWALD, N.M., BAKER, A.R., BERGAMETTI, G., BROOKS, N., DUCE, R.A., JICKELLS, T.D., KUBILAY, N., PROSPERO, J.M., TEGEN, I. (2005) Atmospheric global dust cycle and iron inputs to the ocean. *Global Biogeochemical Cycles* 19, GB4025. <https://doi.org/10.1029/2004GB002402>
- MITRA, S., WASSMANN, R., VLEK, P.L.G. (2005) An appraisal of global wetland area and its organic carbon stock. *Current Science* 88, 25–35. <http://www.jstor.org/stable/24110090>
- MÖCKEL, S.C., ERLENDSSON, E., GÍSLADÓTTIR, G. (2017) Holocene environmental change and development of the nutrient budget of histosols in North Iceland. *Plant and Soil* 418, 437–457. <https://doi.org/10.1007/s11104-017-3305-y>
- MOOSDORF, N., RENFORTH, P., HARTMANN, J. (2014) Carbon dioxide efficiency of terrestrial enhanced weathering. *Environmental Science & Technology* 48, 4809–4816. <https://doi.org/10.1021/es4052022>
- PARISH, F., SIRIN, A., CHARMAN, D., JOOSTEN, H., MINAYEVA, T., SILVIUS, M., STRINGER, L. (2008) *Assessment on Peatlands, Biodiversity and Climate Change: Main Report*. Global Environment Centre, Kuala Lumpur and Wetlands International, Wageningen.
- PARKHURST, D.L., APPELO, C.A.J. (1999) *User's guide to PHREEQC (Version 2): A computer program for speciation, batch-reaction, one-dimensional transport, and inverse geochemical calculations*. Water-Resources Investigations Report 99-4259, US Geological Survey, Denver. <https://doi.org/10.3133/wri994259>
- PETERSEN, G.N., BERBER, D. (2018) Soil temperature measurements in Iceland, status and future outlook vision (in Icelandic: *Jarðvegshitamælingar á Íslandi. Staða númerandi kerfis og framtíðarsýni*). Report of the Icelandic Meteorological Office (*Skiðsla Véðurstofu Íslands*), VI 2018-009, Reykjavík, Iceland. [https://www.vedur.is/media/vedurstofan-utgafa-2018/VI\\_2018\\_009\\_rs.pdf](https://www.vedur.is/media/vedurstofan-utgafa-2018/VI_2018_009_rs.pdf)
- SCHOTT, J., POKROVSKY, O.S., OELKERS, E.H. (2009) The link between mineral dissolution/precipitation kinetics and solution chemistry. *Reviews in Mineralogy* 70, 207–258. <https://doi.org/10.2138/rmg.2009.70.6>
- SHOJI, S., NANZYO, M., DAHLGREN, R. (1995) *Volcanic Ash Soils: Genesis, Properties and Utilization*. Developments in Soil Science, Elsevier, Amsterdam.
- STOCKMANN, U., PADARIAN, J., McBRATNEY, A., MINASNY, B., DE BROGNIEZ, D., MONTANARELLA, L., HONG, S.Y., RAWLINS, B.G., FIELD, D.J. (2015) Global soil organic carbon assessment. *Global Food Security* 6, 9–16 <https://doi.org/10.1016/j.gfs.2015.07.001>
- STREFLER, J., AMANN, T., BAUER, N., KRIEGLER, E., HARTMANN, J. (2018) Potential and costs of carbon dioxide removal by enhanced weathering of rocks. *Environmental Research Letters* 13, 034010. <https://doi.org/10.1088/1748-9326/aaa9c4>
- TAYLOR, L.L., DRISCOLL, C.T., GROFFMAN, P.M., RAU, G.H., BLUM, J.D., BEERLING, D.J. (2021) Increased carbon capture by a silicate-treated forested watershed affected by acid deposition. *Biogeosciences* 18, 169–188. <https://doi.org/10.5194/bg-18-169-2021>
- XU, J., MORRIS, P.J., LIU, J., HOLDEN, J. (2018) PEATMAP: Refining estimates of global peatland distribution based on a meta-analysis. *Catena* 160, 134–140. <https://doi.org/10.1016/j.catena.2017.09.010>



# Direct evidence of CO<sub>2</sub> drawdown through enhanced weathering in soils

T. Linke, E.H. Oelkers, S.C. Möckel, S.R. Gislason

## Supplementary Information

The Supplementary Information includes:

- Soil Classification and Soil Evolution in Iceland
- Detailed Field Site Description
- Details of Field Sampling
- Analytical Methods
- Elemental Analysis
- Calculation of Alkalinity Creation and Export in Our Studied Soil
- Estimated Organic Carbon Storage Within the Studied Soil
- Effect of Basalt on Organic Carbon
- Tables S-1 to S-4
- Supplementary Information References

## Soil Classification and Soil Evolution in Iceland

Iceland is built of volcanic rocks, which are predominantly (80–85 %) of basaltic composition, the remainder being intermediate and silicic volcanics and clastic sediments that are mostly of basaltic composition (Saemundsson, 1979). The oldest exposed rocks are about 15 Myr (McDougall *et al.*, 1984). Iceland was fully covered with glaciers at the Last Glacial Maximum (~20 kyr BP). The ice sheet retreated close to the present coastline around 10.3 kyr BP, and at about 8.0 kyr BP Icelandic glaciers were of similar, or little lesser extent, than at the present (Norðahl *et al.*, 2008). Hence, all Icelandic soils are of Holocene age younger than ~10 kyr BP (Arnalds, 2008).

Andosols are the dominant soils in Iceland, Vitrисols are present in desert areas and organic-rich Histosols are found in some wetland areas (Arnalds, 2008). Andosols are not common in Europe, but they are widespread in the active volcanic areas of the world (Arnalds, 2008). Two main factors are commonly used to classify Icelandic soils: deposition of aeolian (volcanic) material and drainage (Arnalds, 2004). Aeolian material mostly originates from the sandy desert areas located near active volcanic zones or from glaciofluvial outwash plains. After the settlement in Iceland, around 1076 yr BP, the extent of barren areas that are a source for aeolian material significantly increased (Gísladóttir *et al.*,



2008, Dugmore *et al.*, 2009). Andosols are often found in the wetland areas of Iceland where substantial aeolian input is present, lowering the relative organic content, or where some drainage is present, whereas organic-rich Histosols are found in wetlands with little aeolian input. The progression of soil types with improving drainage conditions from wet to dry follows: Histosols (>20 % C), Histic Andosols (12–20 % C), Gleyic Andosols (>1 to <12 % C, poorly drained), and Brown Andosols (>1 to <12 % C, freely drained) and Vitrisol with <1 % organic carbon (Arnalds, 2008). This order also reflects the decreasing distance from the volcanic zones and the source of aeolian materials. The transition between these soil types is fluent, and changes in drainage or aeolian input can lead to a change of the soil type. It is postulated that in absence of the volcanic influences, Icelandic wetland soils would largely be organic Histosols, typical of the arctic environments (Arnalds, 2015, 2008). This suggests that applying enhanced weathering EW by the addition of basaltic dust to an organic-rich Histosol can lead to its transition to a more mineral-rich soil such as an Andosol, as found in our study area.

Histosols or peatlands are classified further as *ombrotrophic* or *minerotrophic*, based on the origin and mineral content of the waters feeding them (Rydin and Jeglum, 2013). While *minerotrophic* soils receive mostly ground water that has interacted with the bedrock upstream, leading to an enrichment of the mineral content in the water, *ombrotrophic* soils are dominantly fed by rainwater, and are therefore nearly free of rock derived dissolved constituents (Rydin and Jeglum, 2013). Our studied field site receives mostly rainwater. Therefore, all dissolved constituents in our soil water are assumed to originate from the interaction of rainwater with the embedded dust of our soil, and the decay of organic matter. Based on this assumption, we compare our data (see Fig. 3) with data from other sites reported in the literature as mostly *ombrotrophic*, implying limited interaction with the underlying bedrocks.

## Detailed Field Site Description

The field site is located above the source of the Rauðalækur (“Red creek”) river at 63° 53' 42.5" N 20° 21' 15.9" W, 7 km north of the town of Hella, South Iceland. This field site has not been used for agriculture or fertilized for at least the past 10 years prior to this study, hence limited anthropogenic contamination is therefore expected. Based on data from the Icelandic Meteorological Office, the average soil temperature is ~7 °C during the summer (Petersen and Berber, 2018). At 100 cm soil depth, the annual maximum temperature is 9 °C and the annual minimum temperature is 1 °C. The soil can, however, temporarily freeze down to a depth of 50 cm (Petersen and Berber, 2018). The annual rainfall in this area is  $1250 \pm 200$  mm. The average storm yields an average of 15 mm of rain with a maximum duration of 20 hours ([www.en.vedur.is/climatology/data](http://www.en.vedur.is/climatology/data)). The surface of the studied soil is hummocky, and the vegetation is characterized by graminoids with a clear predominance of Poaceae. The direction of the groundwater flow, estimated based on the surrounding drainage channels, is towards S/SE. Based on field observations, the groundwater table fluctuates near a depth of 50 cm.

The field site is adjacent to a natural escarpment allowing for the characterization of the subsurface soil profile. Several tephra layers were identified within a cleared vertical face of the escarpment. Layers of organic-rich soil



admixed with air-borne basaltic dust separate the tephra layers. The dust in these layers is finer grained than the basalt in the tephra layers. The tephra layers can be assigned to specific volcanic eruptions, as each volcanic eruption in Iceland has its own chemical fingerprint (Dugmore *et al.*, 2009; Grönvold *et al.*, 1995). These allow determination of the soil accumulation rates. As can be seen in Figure 1b, over the last 3300 years about 220 cm of soil has accumulated, averaging to a soil thickening rate of  $0.067 \text{ cm yr}^{-1}$ . The ‘Settlement layer’, a tephra layer from an eruption of the Vatnajökull volcanic system at  $1079 \pm 2 \text{ BP}$  (Grönvold *et al.*, 1995), which approximately coincides with the initial settlement (Landnám) of Iceland, was barely discernible in the soil profile. Although the exact depth of this Settlement tephra at around 96 cm depth is somewhat uncertain, its location suggests an average soil accumulation rate of  $0.086 \text{ cm yr}^{-1}$  during the last 1120 years. This is consistent with Gísladóttir *et al.* (2011) who reported that the dust flux over South-Central Iceland increased following the emplacement of the Settlement layer. A detailed description of the soil profile is provided in Table S-1 of the Supplementary Information following the guidelines provided in Schoeneberger *et al.* (2012).

## Details of Field Sampling

*In situ* soil waters were sampled 10 m North from the escarpment in the field with suction cup samplers obtained from Prenart, Denmark. Four suction cup samplers were installed into holes drilled at an angle of  $60^\circ$  at depths of 76, 121, 173, 260 cm on 8 November 2017, following the method of Sigfusson *et al.* (2006). The samplers were left in the field over the winter to allow settling of the soil around the samplers and tubing. The first samples from these suction cup samplers were collected during May 2018 and the last were collected November 2018. The suction cup samplers, which are 95 mm long and 21 mm in outer diameter, consist of a 48/52 % mixture of Polytetrafluoroethylene (PTFE) and quartz with an average pore size of  $2 \mu\text{m}$ . These samplers were connected by 1.8 mm inner diameter Teflon (Fluorinated ethylene propylene) tubing to the surface. Four 60-mL syringes located at the surface were connected via 3-way valves and 100 cm long connection polyethylene tubing to the Teflon tubing of the subsurface samplers. The first 30–50 mL of extracted soil water during any sampling was discarded to avoid contamination. It took about 6–8 hours to fill the 60 mL sampling syringes. During the sampling the syringes were kept in a closed cooling box to prevent heating and exposure to sunlight. This approach was adapted to avoid any degassing of the soil solutions and oxidation of the samples. No colour change of the soil solutions due to iron oxidation was observed during the sampling.

Initial sample analysis was performed in the field including sample pH, temperature and Eh measurements, conductivity determination and H<sub>2</sub>S titration. Subsamples for major and trace element analysis via ICP-OES and ICP-MS as well as for ion chromatography to determine Fe<sup>2+</sup>/Fe<sup>3+</sup>, DOC analysis and alkalinity titration were collected and stabilized on site and analysed later in the lab.



## Analytical Methods

The redox potentials ( $E_{\text{meas}}$ ) of the collected fluids were measured directly in the sample syringes in the field using a Microelectrodes Inc MI-800 Micro-ORP Ag/AgCl micro combination redox electrode with a  $\pm 10$  mV uncertainty. These values were converted to equivalent potentials for a standard hydrogen electrode ( $E_{\text{SHE}}$ ) using a +199 mV reference potential,  $E^\circ$ , for the Ag/AgCl electrode (Sawyer *et al.*, 1995). This calculation was performed using the Nernst equation:

$$E_{\text{SHE}} = E_{\text{meas}} + \ln(10) \cdot (R \cdot T) / F \cdot \text{pH} + E^\circ_{\text{Ag/AgCl}},$$

where  $R$  refers to the gas constant,  $F$  designates the Faraday's constant, and  $T$  symbolizes the temperature in kelvin. Subsequently, ~5 mL of each sampled fluid was transferred into 10 mL polypropylene vials for pH, temperature, dissolved oxygen, and conductivity measurement. The pH was measured using a Eutech pH 6+ electrode with an uncertainty of  $\pm 0.01$  pH units. The dissolved oxygen and conductivity of the samples were measured using a Micro electrodes MI-730 Micro-Oxygen Electrode with an uncertainty of  $\pm 0.5$  % and a Eutech COND 6+ with an uncertainty of  $\pm 10$   $\mu$ S, respectively. For major and trace element analysis, 10 mL of each fluid sample was first filtered through 0.2  $\mu$ m cellulose acetate in-line filters then transferred into acid washed polypropylene bottles. A small quantity of 65 % Merck suprapure HNO<sub>3</sub> was added to acidify these samples to 0.5 % HNO<sub>3</sub>. Samples for iron speciation measurement were first filtered through 0.2  $\mu$ m cellulose acetate in-line filters then placed into acid cleaned polypropylene bottles. Merck HCl was added to these samples to attain a final acid concentration of 0.5 %. Samples for dissolved organic carbon analysis were collected in acid washed polycarbonate bottles and acidified with 0.5 M suprapure, Merck HCl to a final acid concentration of 3.3 %.

Dissolved hydrogen sulphide, H<sub>2</sub>S, was determined in the field by precipitation titration immediately after sampling with an uncertainty of  $\pm 0.7$   $\mu$ mol kg<sup>-1</sup>, using mercury acetate solution Hg(CH<sub>3</sub>COO)<sub>2</sub> of a known concentration as described by Arnórsson (2000). Alkalinity titrations were performed immediately after returning the samples to the laboratory. For each titration, ~5 mL of fluid was transferred in a 10 mL vial and titrated to pH 3.3 by addition of 0.1 M HCl while constantly stirring the fluid. The pH of the fluid was recorded using a glass pH electrode together with a pH 110, Eutech instruments millivolt meter. The alkalinity was calculated by the Gran method using the inflection points (Gran, 1952). The final measured alkalinity values are given in meq kg<sup>-1</sup> with an uncertainty of  $\pm 5$  % or less.

## Elemental Analysis

Major element compositions of all fluid samples were determined using a Ciros Vision, Spectro Inductively Coupled Plasma Optical Emission Spectrometer (ICP-OES). The instrument was calibrated using the SEL-11 in-house standard, which was referenced to the SPEX CertiPrep commercial standard material. All standards and measured samples were acidified to 0.5 % using suprapure HNO<sub>3</sub> prior to analysis. All measurements were run in duplicate. Blank solutions were measured after every 5 samples and uncertainties were below  $\pm 5$  % for each element.



Iron species were determined using a Dionex 3000 ion chromatography system equipped with a Variable Wavelength Detector using the method described by Kaasalainen *et al.* (2016). This method separates  $\text{Fe}^{2+}$  and  $\text{Fe}^{3+}$  using pyridine-2,6-dicarboxylic acid (PDCA) as a chelating agent. It detects the distinct Fe cations by post-column derivatization using 4-(2-pyridylazo)resorcinol with a peak absorbance at 530 nm, a detection limit of  $\sim 2 \mu\text{g L}^{-1}$  and an uncertainty of  $\pm 2\%$  or less for  $\text{Fe}^{2+}$  and  $\pm 10\%$  for  $\text{Fe}^{3+}$  for 200–1000  $\mu\text{L}$  samples.

Dissolved organic carbon concentrations were determined by size exclusion chromatography using a Liquid Chromatography – Organic Carbon Detection system (LC-OCD) obtained from DOC Labor in Karlsruhe, Germany, following the method of Huber *et al.* (2011). The system was calibrated for the molecular masses of humic and fulvic acids using standard material from the Suwannee River, provided by the International Humic Substances Society (IHSS). All DOC measurements have an uncertainty of 5 % or less.

## Calculation of Alkalinity Creation and Export in Our Studied Soil

Alkalinity export in our field site was determined by multiplying the mass of water passing through the soil by the alkalinity generated in the soil, taking account the loss of alkalinity as the soil solution interacted with the atmosphere. Any effect of eventual changes in this alkalinity after the fluids arrive in the oceans is not taken into account. The alkalinity of the soil solution after its equilibration with the atmosphere was calculated using the PHREEQC software version 3.4.0 (Parkhurst and Appelo, 1999) together with the minteq.v4 thermodynamic database (Allison *et al.*, 1991; US Environmental Protection Agency, 1998). This alkalinity was determined from the average of all measured major element concentrations, pH and alkalinity in the deepest soil water samplers (see Table S-2). This fluid was equilibrated with atmospheric  $\text{O}_2$  concentration. Ferrihydrite is allowed to precipitate at local equilibrium as the fluid oxidized. The resulting fluid was then equilibrated with the 400 ppm  $\text{CO}_2$  concentration of the atmosphere to account for fluid degassing.

The mass of fluid passing through the soil was estimated to be equal to the difference between the mean precipitation for the field site minus the evapotranspiration and the direct runoff. The mean precipitation is equal to  $1250 \pm 200 \text{ mm yr}^{-1}$ , based on the records from the measurement station in Hella located  $\sim 7 \text{ km}$  away from the field site operated by the Icelandic Metrological Office Veðurstofa Íslands (<https://en.vedur.is/climatology/data>). The evapotranspiration at the field site was estimated based on Jóhannesson *et al.* (2007) to be equal to 16 % of the precipitation corresponding to  $200 \text{ mm yr}^{-1}$ . The direct surface runoff is estimated to be 10 %, based on data published by Sigurðsson *et al.* (2004). After subtracting the evapotranspiration and direct surface runoff, approximately  $925 \pm 150 \text{ kg m}^{-2} \text{ yr}^{-1}$  of water are estimated to pass through the studied soil annually.

The soil water alkalinity in the deep soil was  $2.59 \pm 0.34 \text{ meq kg}^{-1}$  based on the average of the measurements at 260 cm depth. The average alkalinity for the surface waters after oxidation and the precipitation of ferrihydrite calculated with PHREEQC is  $1.53 \pm 0.2 \text{ meq kg}^{-1}$ . Note that the oxidation from  $\text{Fe}^{2+}$  to  $\text{Fe}^{3+}$  releases  $\text{H}^+$ . The consequential formation of ferrihydrite from the  $\text{Fe}^{3+}$  releases additional  $\text{H}^+$ , decreasing the pH and alkalinity as well as decreasing



$\text{CO}_2$  solubility. Multiplying this  $1.53 \pm 0.2 \text{ meq kg}^{-1}$  average alkalinity value by the estimated annual water flux through the soil yields an annual alkalinity export *via* surface waters of  $1.45 \pm 0.3 \text{ eq m}^{-2} \text{ yr}^{-1}$ . Multiplying this number by the atomic weight of carbon yields an annual carbon flux of  $17 \pm 3.6 \text{ g m}^{-2} \text{ yr}^{-1}$  or  $0.17 \pm 3.6 \text{ t ha}^{-1} \text{ yr}^{-1}$  of C. Note the long-term fate of this captured carbon may evolve once the river water transporting this carbon arrives in the oceans. It should be emphasized that the alkalinity drawn down by the increasing alkalinity could include some contribution from decaying organic material in the soil column. This carbon was originally removed from the atmosphere by photosynthesis, so contributes to the carbon drawdown from the atmosphere as does the direct dissolution of  $\text{CO}_2$  from the atmosphere.

To extrapolate the annual mass of carbon drawdown to the gigaton scale, we divided one gigaton of  $\text{CO}_2$ , which is equal to  $2.73 \times 10^8$  tons of C by the  $0.17 \text{ t ha}^{-1} \text{ yr}^{-1}$  of C drawdown in rivers provoked by the addition of basaltic dust to our field site. This yielded a surface area of  $1.6 \times 10^9 \text{ ha}$ . This surface area is equal to  $1.6 \times 10^7 \text{ km}^2$ . This is larger than the surface area of the United States, which is equal to  $9.8 \times 10^6 \text{ km}^2$ . The mass of dust needed to be added to  $1.6 \times 10^7 \text{ km}^2$  annually to attain the same  $500\text{--}800 \text{ g m}^{-2} \text{ yr}^{-1}$  of dust added to our study site is obtained by multiplying this flux and surface area. This calculation yields 8 to  $13 \times 10^9 \text{ t yr}^{-1}$ , which equals 8 to 13 Gt  $\text{yr}^{-1}$ .

One additional caveat to applying alkalinity generation from enhanced weathering of soils on the continents to global carbon drawdown from the atmosphere is the fate of soil generated alkalinity after its transport in rivers to the oceans. The exact mass of  $\text{CO}_2$  removed from the oceans due to alkalinity input is currently debated, but is likely attenuated by carbonate mineral precipitation (Renforth and Henderson, 2017; Moras *et al.*, 2022; Hartmann *et al.*, 2023). Recent estimates suggest a  $\text{CO}_2$  uptake efficiency of only 0.6 to 0.8 mol of  $\text{CO}_2$  for each mole of alkalinity added to the oceans (He and Tyka, 2023). Such observations suggest that the total carbon drawdown from the atmosphere by alkalinity generation on the continents will depend on the eventual fate of this alkalinity and it is likely decreased by marine processes.

## Estimated Organic Carbon Storage Within the Studied Soil

A substantial mass of carbon is stored by soils in organic material. The rate of organic carbon buildup in our studied soil can be estimated by taking account of the rate of soil formation and the organic content of this soil. The average soil formation rate at our study site is estimated to be  $0.067 \text{ cm yr}^{-1}$ . This estimate is made by dividing the current 2.2 m soil thickness by 3300 years, the time the soil developed (see Fig. 1). The organic carbon content of the studied Histic/Gleyic Andosol is between ~12 % and 20 % of the dry mass and it has a porosity between 50 % and 75 % (Snæbjörnsson, 1982; Orradottir *et al.*, 2008). The mass of organic carbon in our studied soil was estimated by considering it is comprised of two parts, an upper part formed after the settlement (1076 yr BP) and a lower part formed from 1076 down to 3300 yr BP (Fig. 1). This separation is based on the report of an increase in dust flux after this time (Gísladóttir *et al.*, 2008; Dugmore *et al.*, 2009). These parts are divided based on the position of tephra layers that allow the direct determination of the net rates of soil accumulation, including the effects of soil erosion, over time. The upper part is a Gleyic Andosol containing



<12 % C by dry weight extending down to ~90 cm, while the lower part is a Histic Andosol containing 12–20 % C by dry weight from ~90 to 218 cm. These maximum soil carbon values of 12 and 20 % were multiplied by the height of each soil section, assuming a porosity between 50 and 75 % (Snæbjörnsson, 1982; Orradottir *et al.*, 2008) to estimate the total carbon present in the studied soil. The combination of this range of carbon content and porosity values yield an estimated total mass of organic carbon stored in this soil equal to 86–172 kg C m<sup>-2</sup>. The total mass of carbon estimated in our study area compares well with corresponding estimates of Óskarsson *et al.* (2004), who estimate the C stocks of Histosols in Iceland to be on average 197 kg C m<sup>-2</sup>, and the more mineral-rich Histic Andosols in Iceland to be 89 kg C m<sup>-2</sup>. Further details of this calculation are provided in Table S-4. Dividing this mass by the 3300-year age of the soil column yields an average organic carbon production rate of 26–52 gC m<sup>-2</sup> yr<sup>-1</sup>. Note that the mass of carbon in organic material, reported in units of mass of C can be converted to the equivalent mass CO<sub>2</sub> by multiplying the former by the ratios of their respective molar masses: 44/12.

## Effect of Basalt on Organic Carbon

The degree to which the addition of basalt increases or decreases the total mass of organic carbon in a soil is currently poorly constrained. Vicca *et al.* (2022) argued that the efficiency of enhanced weathering effort is governed by biologic processes. These authors noted that nutrients released by the addition of ground rocks to soils could enhance plant growth and promote organic carbon storage in soils. They also postulated that the addition of this material could accelerate organic material decay in the subsurface. Goll *et al.* (2021) suggested that the addition of basalt to soils would improve the fertility potentially, enhancing organic carbon storage in soils. Some supporting evidence was reported by Angst *et al.* (2018), who observed that soils derived from a basaltic rock stored more organic carbon than soils derived from sandstone or from loess. This was interpreted by these authors to be due to a combination of a higher clay content and greater availability of nutrients in the basalt derived soils. Similarly, da Silva *et al.* (2016) concluded that the organic carbon content of soils derived from granitic rocks increased with increasing mafic content of the parent rock due to increased clay mineral content. Möckel *et al.* (2021a, 2021b) provided evidence that volcanic mineral dust, and soil and tephra layers hamper organic carbon decomposition in Histosols of natural peatlands in Iceland. In contrast, other studies found that soil parent material and mineral oxide compositions have little effect on the mass of organic carbon in soils (Araujo *et al.*, 2017). One factor that is clearly detrimental to the preservation of soil organic carbon is tilling. Soil tilling has been shown to accelerate greatly soil organic carbon degradation (Wang *et al.*, 2020; Shakoor *et al.*, 2021; Li *et al.*, 2023). Such observations suggest that the way that basaltic dust is added to soil during enhanced weathering efforts may be critical for increasing the net carbon drawdown in these soils. In either case, consideration of the relative rates of carbon drawdown through inorganic compared to organic processes presented in this study suggests that the latter may dominate the net carbon storage in soils due to enhanced weathering. This makes the quantification of the role of basaltic dust on productivity and organic preservation a critical factor in optimizing enhanced weathering efforts.



## Supplementary Tables

**Table S-1** Description of the soil profile depicted in Figure 1a and 1b. Profile description following Schoeneberger *et al.* (2012). Note that O horizons are here defined as layers with an estimated carbon content  $\geq 12\%$ .

Horizon	Depth (cm)	Roots (quantity and size) <sup>1</sup>	Boundary (distinctness, topography) <sup>2</sup>	Structure (grade, size, type) <sup>3</sup>	(grade, Mottles (quantity and size) <sup>4</sup>	Soil colour (moist; Munsell colour code)	Comments
A (O)	0–23	3 vf, 2 f, 2 m	G, S	3, f, sbk	f1	2.5YR 3/4	
2O1	23–35	3 vf, 2 f, 1 m	C, W	2, f, abk	f1	7.5YR 2.5/2;	
2O2	35–58	3 vf, 1 f, 1 m 1 vf, very few f, very few co	C, W G, B	2, tn, pl t, m, sbk	–	towards 2.5YR 4/3 in the lower half of the horizon Gradual downwards colour change from 10YR 3/3 to 7.5YR 2.5/3	
2O3	58–71	very few vf, 1 co	A, W	1, m, abk	m 5	7.5YR 2.5/2 (main horizon colour); 7.5YR 4/6 (mottles)	
2O4	71–96	2 vf, 1 f, 1 co	A, W	7.5 YR 4/6	100.5–101.5 cm: coarse grey beige coloured tephra		
2O5	96–114.5	3 vf, very few f, 1 co	A, W	2, f, sbk	c 2, c 3	7.5YR 2.5/1	
2O6	116.5–133	3 vf	A, W	2, m, pl	f1	124.5–125 cm: dark basaltic tephra	
2O7	133–137	3 vf	A, W	2, m, gr	f2	Layer of rather coarse material; might for instance be from a flooding event	
3C – T	137–139.5						
4O	139.5–162	3 vf, 1 f, f co	A, W	2, tk, pl	–	dark basaltic tephra	
5C – T	162–164.5					wood remains in the lower half of the horizon (o: c. 1.5–4 cm)	
6O	164.5–182	3 vf	A, W	1, m, pl	–	very coarse dark-light tephra	
7C – T	182–187.5 187.5–2018 the ditch)	3 vf, 1 f (bottom of the ditch)	not applicable, bottom of the ditch	2 tk pl	7.5YR 2.5/1	wood remains (quite evenly distributed; o: c. 1.5 cm)	
8O					7.5YR 2/2	dark basaltic tephra	
						Wood remains ( $\sigma \leq c. 2\text{cm}$ )	Wood remains ( $\sigma \leq c. 2\text{cm}$ )

<sup>1</sup> vf-very fine, f-fine, m-medium, co-coarse; <sup>2</sup> A-abrupt, C-clear, G-gradual, S-smooth, W-wavy, B-broken; <sup>3</sup> f-fine, tn-fine(thin), m-medium, dk-coarse, sbk-subangular blocky, abk-angular blocky, pl-platy, granular; <sup>4</sup> f-few, m-many, c-common.



**Table S-2** Soil water compositions measured in the present study.

Sample	Date	Depth (cm)	T (°C)	pH	Eh <sub>SHE</sub> (mV)	Alk (meq kg <sup>-1</sup> )	DIC (mmol kg <sup>-1</sup> )	DOC (μmol kg <sup>-1</sup> )	Major element concentrations (μmol kg <sup>-1</sup> )									
									Si	Na	K	Ca	Mg	S(tot) <sup>-</sup>				
LOQ <sup>1</sup>									4.0	11	3.0	1.0	0.2	6.0	28	0.28	0.1	0.1
1*	23 May 2018	76	9	5.84	233	1.48			678	449	7	420	402	97	402	0.93		
2*		121	9	6.27	-9				716	435	13	427	379	102	357	0.99		
3*		173	8.9	6.35	-8				717	390	14	293	233	79	350	1.25		
4*		260	10.1	6.37	-57	2.3			644	441	20	513	535	7	284	2.81		
1a	21 June 2018	76	19.7	6.02	451	1.41	4.45	247	678	464	<LOQ	380	359	90	404	<LOQ	0.7	
2a		121	19	6.21	116	1.56	3.72	252	797	427	17	334	261	99	287	2.18	371	10.2
3a		173	19.2	6.2	106	1.53	3.67	344	778	435	<LOQ	384	340	47	322	2.64	460	12.1
4a		260	24.8	6.25	71	2.21	4.75	233	722	448	16	522	527	<LOQ	295	2.57	562	24.9
1b	14 Aug 2018	76	16.8	6.06	298	1.5	4.57	381	761	471	0	381	361	71	300	<LOQ	<LOQ	0.7
2b		121	15.9	6.18	76	1.38	3.50	258	860	446	19	365	314	120	255	2.63	415	25.7
3b		173	15.2	6.28	88	1.59	3.55	265	802	456	16	374	341	29	280	2.62	388**	86.4**
4b		260	15.4	6.41	66	2.13	4.05	740	581	57	486	515	27	462	2.63	464	464	93.9
1c	18 Sep 2018	76	7.6	6	287	1.5	5.47	418	772	482	<LOQ	378	358	111	206	1.70	0.4	0.9
2c		121	8.9	6.22	123	2.34	5.85	339	887	450	19	422	342	124	254	2.96	412	78.5
3c		173	8.2	6.19	112	2.5	6.53	344	810	463	16	387	348	20	293	2.55	391	74.5
4c		260	7.5	6.28	85	3.02	7.04	331	747	446	22	487	493	<LOQ	282	2.64	451	86.0
1d	29 Oct 2018	76	22.5	5.98	439	0.83	2.73	382	566	449	22	330	310	101	583	<LOQ	0.8	
2d		121	22.5	6.13	229	1.56	4.04	488	732	416	20	323	269	77	492	2.13	364	12.0
3d		173	22.5	6.18	224	2.16	5.20	329	807	453	14	383	354	57	332	2.33	465	9.8
4d		260	22.5	6.39	179	2.8	5.20	366	755	444	19	494	499	14	328	2.47	535	24.5
1e	21 Nov 2018	76	22.6	5.85	429	1.08	4.40	650	450	17	343	333	106	446	1.54	<LOQ	0.6	
2e		121	22.6	6.11	282	1.21	3.24		668	354	36	229	190	50	368	2.11	246	12.5
3e		173	22.6	6.15	255	2.17	5.45		794	435	17	351	327	44	349	2.76	438	13.6
4e		260	22.6	6.28	190	2.78	5.88		730	423	20	442	451	<LOQ	309	2.53	506	20.7

<sup>1</sup> Limit of Quantification.\* Sample not used for modelling due to missing analysis.  
\*\* Fe species calculated from Fe<sub>tot</sub> and measured Eh.

**Table S-3** Literature data included in Figure 3.

<b>pH</b>	<b>Alkalinity (meq kg<sup>-1</sup>)</b>	<b>Classification</b>	<b>Reference</b>	<b>Location</b>
3.96 3.93 5.38 5.44 6.28 6.21 6.00 5.93	0 0 0.198 0.371 0.764 0.743 0.623 0.695	Bog  Poor fen  Forested moderately rich fen  Open moderately rich fen	Vitt <i>et al.</i> (1995)	Central Alberta, Canada
5.17 5.33	0.055 0.01	Not specified	Dawson <i>et al.</i> (2002)	NE Scotland, United Kingdom Mid Wales, United Kingdom
5.46 4.68 4.74 4.52	0.5 0.2 0 0	Minerotrophic lawns Ombrotrophic carpets Ombrotrophic lawns Ombrotrophic hummocks	Bragazza <i>et al.</i> (2005)	Wölfl Moor, South Tyrol, Italy
5.04 3.76 3.75 3.68	0.7 0 0 0	Minerotrophic lawns Ombrotrophic carpets Ombrotrophic lawns Ombrotrophic hummocks	Bragazza <i>et al.</i> (2005)	Ryggmossen, Uppsala, Sweden
4.2 4.17 4.66	0.02 0.02 0.076	Bog water	Kulzer <i>et al.</i> (2001)	Western Washington, King County, USA
3.6 6.5	0 1.082	Ombrotrophic bog Groundwater fen	Verry (1975)	Minnesota, USA



**Table S-4** Estimates of the carbon stock of the field site and annual accumulation rates with varying porosity.

Depth	75 % porosity		50 % porosity	
	0–90 cm soil	90–218 cm soil	0–90 cm soil	90–218 cm soil
cm of tephra (zero organic carbon)	—	10 cm	—	10 cm
C content	12 %	20 %	12 %	20 %
Soil height	90 cm	118 cm	90 cm	118 cm
Soil mass	225 kg m <sup>-2</sup>	295 kg m <sup>-2</sup>	450 kg m <sup>-2</sup>	590 kg m <sup>-2</sup>
mass organic carbon	27 kg C m <sup>-2</sup>	59 kg C m <sup>-2</sup>	54 kg C m <sup>-2</sup>	118 kg C m <sup>-2</sup>
<b>Total C stored</b>	<b>86 kg C m<sup>-2</sup></b>		<b>172 kg C m<sup>-2</sup></b>	
Timespan	1140 years	2180 years	1140 years	2180 years
C accumulation rate	0.024 kg C m <sup>-2</sup> yr <sup>-1</sup>	0.027 kg C m <sup>-2</sup> yr <sup>-1</sup>	0.047 kg C m <sup>-2</sup> yr <sup>-1</sup>	0.054 kg C m <sup>-2</sup> yr <sup>-1</sup>



## Supplementary Information References

- Allison, J.D., Brown, D.S., Novo-Gradac, K.J. (1991) MINTEQA2/PRODEFA2, *A geochemical assessment model for environmental systems: version 3.0 user's manual*. Environmental Research Laboratory Office of Research and Development U.S. Environmental Protection Agency, Athens, Georgia.
- Angst, G., Messinger, J., Greiner, M., Häusler, W., Hertel, D., Kirfel, K., Kögel-Knabner, I., Leuschner, C., Rethemeyer, J., Mueller, C.W. (2018) Soil organic carbon stocks in topsoil and subsoil controlled by parent material, carbon input in the rhizosphere, and microbial-derived compounds. *Soil Biology and Biochemistry* 122, 19–30. <https://doi.org/10.1016/j.soilbio.2018.03.026>
- Araujo, M.A., Zinn, Y.L., Lal, R. (2017) Soil parent material, texture and oxide contents have little effect on soil organic carbon retention in tropical highlands. *Geoderma* 300, 1–10. <https://doi.org/10.1016/j.geoderma.2017.04.006>
- Arnalds, O. (2004) Volcanic soils of Iceland. *Catena* 56, 3–20. <https://doi.org/10.1016/j.catena.2003.10.002>
- Arnalds, O. (2008) Soils of Iceland. *Jökull* 58, 409–421. <https://doi.org/10.33799/jokull2008.58.409>
- Arnalds, O. (2015) *The Soils of Iceland*. World Soils Book Series, Springer, Dordrecht. <https://doi.org/10.1007/978-94-017-9621-7>
- Arnórsson, S. (2000) *Isotopic and Chemical Techniques in Geothermal Exploration, Development and Use*. International Atomic Energy Agency, Vienna.
- Bragazza, L., Rydin, H., Gerdol, R. (2005) Multiple gradients in mire vegetation: A comparison of a Swedish and an Italian bog. *Plant Ecology* 177, 223–236. <https://www.jstor.org/stable/20146727>
- Da Silva, Y.J.A.B., do Nascimento, C.W.A., Biondi, C M., van Straaten, P., de Souza Jr., V.S., Ferreira, T.O. (2016) Weathering rates and carbon storage along a climosequence of soils developed from contrasting granites in northeast Brazil. *Geoderma* 284, 1–12. <https://doi.org/10.1016/j.geoderma.2016.08.009>
- Dawson, J.J.C., Billett, M.F., Neal, C., Hill, S. (2002) A comparison of particulate, dissolved and gaseous carbon in two contrasting upland streams in the UK. *Journal of Hydrology* 257, 226–246. [https://doi.org/10.1016/S0022-1694\(01\)00545-5](https://doi.org/10.1016/S0022-1694(01)00545-5)
- Dugmore, A.J., Gísladóttir, G., Simpson, I.A., Newton, A. (2009) Conceptual Models of 1200 Years of Icelandic Soil Erosion Reconstructed Using Tephrochronology. *Journal of the North Atlantic* 2, 1–18. <https://doi.org/10.3721/037.002.0103>
- Gísladóttir, G., Erlendsson, E., Lal, R., Bigham, J. (2008) Erosional effects on terrestrial resources over the last millennium in Reykjanes, southwest Iceland. *Quaternary Research* 73, 20–32. <https://doi.org/10.1016/j.yqres.2009.09.007>
- Gísladóttir, G., Erlendsson, E., Lal, R. (2011) Soil evidence for historical human-induced land degradation in West Iceland. *Applied Geochemistry* 26, 2009–2012. <https://doi.org/10.1016/j.apgeochem.2011.03.021>
- Goll, D.S., Ciais, P., Amann, T., Buermann, W., Chang, J., Eker, S., Hartmann, J., Janssens, I., Li, W., Obersteiner, M., Penuelas, J., Tanaka, K., Vicca, S. (2021) Potential CO<sub>2</sub> removal from enhanced weathering by ecosystem



- responses to powdered rock. *Nature Geoscience* 14, 545–549. <https://doi.org/10.1038/s41561-021-00798-x>
- Gran, G. (1952) Determination of the equivalence point in potentiometric Titrations. Part II. *Analyst* 77, 661–671. <https://doi.org/10.1039/AN9527700661>
- Grönvold, K., Óskarsson, N., Johnsen, S.J., Clausen, H.B., Hammer, C.U., Bond, G., Bard, E. (1995) Ash layers from Iceland in the Greenland GRIP ice core correlated with oceanic and land sediments. *Earth and Planetary Science Letters* 135, 149–155. [https://doi.org/10.1016/0012-821X\(95\)00145-3](https://doi.org/10.1016/0012-821X(95)00145-3)
- Hartmann, J., Suitner, N., Lim, C., Schneider, J., Marín-Samper, L., Arístegui, J., Renforth, P., Taucher, J., Riebsell, U. (2023) Stability of alkalinity in ocean alkalinity enhancement (OAE) approaches-consequences for durability of CO<sub>2</sub> storage. *Biogeosciences* 20, 781–802. <https://doi.org/10.5194/bg-20-781-2023>
- He, J., Tyka, M.D. (2023) Limits and CO<sub>2</sub> equilibration of near-coast alkalinity enhancement. *Biogeosciences* 20, 27–43. <https://doi.org/10.5194/bg-20-27-2023>
- Huber, S.A., Balz, A., Abert, M., Pronk, W. (2011) Characterisation of aquatic humic and non-humic matter with size-exclusion chromatography – organic carbon detection – organic nitrogen detection (LC-OCD-OND). *Water Research* 45, 879–885. <https://doi.org/10.1016/j.watres.2010.09.023>
- Jóhannesson, T., Aðalgeirs Þóttir, G., Björnsson, H., Crochet, P., Elíasson, E.B., Sverrir Guðmundsson, S., Jónsdóttir, J.F., Ólafsson, H., Pálsson, F., Rögnvaldsson, O., Sigurðsson, O., Snorrason, A., Sveinsson, O.G.B., Thorsteinsson, T. (2007) *Effect of climate change on hydrology and hydro-resources in Iceland*. National Energy Authority - Hydrological Service Technical Report OS-2007/011, 91.
- Kaasalainen, H., Stefánsson, A., Druschel, G.K. (2016) Determination of Fe(II), Fe(III) and Fe<sub>total</sub> in thermal water by ion chromatography spectrophotometry (IC-Vis). *International Journal of Environmental Analytical Chemistry* 96, 1074–1090. <https://doi.org/10.1080/03067319.2016.1232717>
- Kulzer, L., Luchessa, S., Cooke, S., Errington, R., Weinmann, F. (2001) *Characteristics of the Low-Elevation Sphagnum-Dominated Peatlands of Western Washington: A Community Profile Part 1: Physical, Chemical and Vegetation Characteristics*. Report to U.S. Environmental Protection Agency. King County Department of Natural Resources, Seattle.
- Li, Z., Zhang, Q., Li, Z., Qiao, Y., Du, K., Yue, Z., Tian, C., Leng, P., Cheng, H., Chen, G., Li, F. (2023) Responses of soil greenhouse gas emissions to no-tillage: A global meta-analysis. *Sustainable Production and Consumption* 36, 479–492. <https://doi.org/10.1016/j.spc.2023.02.003>
- McDougall, I., Kristjansson, L., Saemundsson, K. (1984) Magnetostratigraphy and Geochronology of Northwest Iceland. *Journal of Geophysical Research: Solid Earth* 89, 7029–7060. <https://doi.org/10.1029/JB089iB08p07029>
- Möckel, S.C., Erlendsson, E., Gísladóttir, G. (2021a) Andic Soil Properties and Tephra Layers Hamper C Turnover in Icelandic Peatlands. *Journal of Geophysical Research: Biogeosciences* 126, e2021JG006433. <https://doi.org/10.1029/2021JG006433>
- Möckel, S.C., Erlendsson, E., Prater, I., Gísladóttir, G. (2021b) Tephra deposits and carbon dynamics in peatlands of a



- volcanic region: Lessons from the Hekla 4 eruption. *Land Degradation and Development* 32, 654–669. <https://doi.org/10.1002/ldr.3733>
- Moras, C.A., Bach, L.T., Cyronak, T., Joannes-Boyau, R., Schulz, K.G. (2022) Ocean alkalinity enhancement-avoiding runaway CaCO<sub>3</sub> precipitation during quick and hydrated lime dissolution. *Biogeosciences* 19, 3537–3557. <https://doi.org/10.5194/bg-19-3537-2022>
- Norðdahl, H., Ingólfsson, Ó., Pétursson, H.G., Hallsdóttir, M. (2008) Late Weichselian and Holocene environmental history of Iceland. *Jökull* 58, 343–364. <http://dx.doi.org/10.33799/jokull2008.58.343>
- Orradottir, B., Archer, S.R., Arnalds, O., Wilding, L.P., Thurow, T.L. (2008) Infiltration in Icelandic Andisols: The Role of Vegetation and Soil Frost. *Arctic, Antarctic and Alpine Research* 40, 412–421. [https://doi.org/10.1657/1523-0430\(06-076\)\[ORRADOTTIR\]2.0.CO;2](https://doi.org/10.1657/1523-0430(06-076)[ORRADOTTIR]2.0.CO;2)
- Óskarsson, H., Arnalds, Ó., Gudmundsson, J., Gudbergsson, G. (2004) Organic carbon in Icelandic Andosols: Geographical variation and impact of erosion. *Catena* 56, 225–238. <https://doi.org/10.1016/j.catena.2003.10.013>
- Parkhurst, D.L., Appelo, C.A.J. (1999) *User's guide to PHREEQC (Version 2): A computer program for speciation, batch-reaction, one-dimensional transport, and inverse geochemical calculations*. Water-Resources Investigations Report 99-4259, US Geological Survey, Denver. <https://doi.org/10.3133/wri994259>
- Petersen, G.N., Berber, D. (2018) Soil temperature measurements in Iceland, status and future outlook (in Icelandic: *Jarðvegshitamælingar á Íslandi. Staða núverandi kerfis og framtíðarsýn*). Report of the Icelandic Meteorological Office (Skýrsla Veðurstofu Íslands), VI 2018-009, Reykjavík, Iceland. [https://www.vedur.is/media/vedurstofan-utgafa-2018/VI\\_2018\\_009\\_rs.pdf](https://www.vedur.is/media/vedurstofan-utgafa-2018/VI_2018_009_rs.pdf)
- Renforth, P., Henderson, G. (2017) Assessing ocean alkalinity for carbon sequestration. *Reviews of Geophysics* 55, 636–674. <https://doi.org/10.1002/2016RG000533>
- Rydin, H., Jeglum, J.K. (2013) *The Biology of Peatlands*. Second Edition, Biology of Habitats Series, Oxford University Press, Oxford. <https://doi.org/10.1093/acprof:osobl/9780199602995.001.0001>
- Saemundsson, K. (1979) Outline of the geology of Iceland. *Jökull* 29, 7–28. <https://doi.org/10.33799/jokull1979.29.007>
- Sawyer, D.T., Roberts, J.L., Sobkowiak, A. (1995) *Electrochemistry for chemists*. Second Edition, Wiley, New York.
- Schoeneberger, P.J., Wysocki, D.A., Benham, E.C., Soil Survey Staff (2012) *Field Book for Describing and Sampling Soils*, version 3.0. Natural Resources Conservation Service, U.S. Department of Agriculture, National Soil Survey Center, Lincoln, NE.
- Shakoor, A., Shahbaz, M., Farooq, T.H., Sahar, N.E., Shahzad, S.H., Altaf, M.M., Ashraf, M. (2021) A global meta-analysis of greenhouse gases emission and crop yield under no-tillage as compared to conventional tillage. *Science of the Total Environment* 750, 142299. <https://doi.org/10.1016/j.scitotenv.2020.142299>
- Sigfusson, B., Paton, G.I., Gislason, S.R. (2006) The impact of sampling techniques on soil pore water carbon measurements of an Icelandic Histic Andosol. *Science of the Total Environment* 369, 203–219. <https://doi.org/10.1016/j.scitotenv.2006.01.012>
- Sigurðsson, B.D., Bjarnadottir, B., Strachan, I., Palmason, F. (2004) The experimental forest in Gunnarsholt II - Water



in the forest (in Icelandic: *Tilraunaskógrinn í Gunnarsholti II – Vatnið í skóginum*). *The Forestry Journal* (In Icelandic: *Skógræktarritið*) 1, 55–64.

Snæbjörnsson, Á. (1982) *Review of soil hydraulic conductivity measurements in Borgarfjörður, Iceland* (in Icelandic: *Um Vatnsleiðnimælingar í Jarðvegi á nokkrum stöðum í Borgarfirði*), Report number 45-1982. <https://vatnsidnadur.net/wp-content/uploads/2017/05/45.-Um-vatnsleiðnimælingar-á-nokkrum-stöðum-í-Borgarfirði.-BÁH.pdf>

U.S. Environmental Protection Agency (1998) MINTEQA2/PRODEFA2, A Geochemical Assessment Model for Environmental Systems: User Manual Supplement for Version 4.0. vol. 1998.

Verry, E. (1975) Streamflow Chemistry and Nutrient Yields from Upland-Peatland Watersheds in Minnesota. *Ecology* 56, 1149–1157. <https://doi.org/10.2307/1936154>

Vicca, S., Goll, D.S., Hagens, M., Hartmann, J., Janssens, I.A., Neubeck, A., Peñuelas, J., Poblador, S., Rijnders, J., Sardans, J., Struyf, E., Swoboda, P., van Groenigen, J.W., Vienne, A., Verbruggen, E. (2022) Is the climate change mitigation effect of enhanced silicate weathering governed by biological processes? *Global Change Biology* 28, 711–726. <https://doi.org/10.1111/gcb.15993>

Vitt, D.H., Bayley, S.E., Jin, T.-L. (1995) Seasonal variation in water chemistry over a bog-rich fen gradient in Continental Western Canada. *Canadian Journal of Fisheries and Aquatic Sciences* 52, 587–606. <https://doi.org/10.1139/f95-059>

Wang, H., Wang, S., Yu, Q., Zhang, Y., Wang, R., Li, J., Wang, X. (2020) No tillage increases soil organic carbon storage and decreases carbon dioxide emission in the crop residue-returned farming system. *Journal of Environmental Management* 261, 110261. <https://doi.org/10.1016/j.jenvman.2020.110261>

